Journal of Alloys and Compounds 488 (2009) 414–419

Contents lists available at ScienceDirect

Journal of Alloys and Compounds

journal homepage: www.elsevier.com/locate/jallcom

Improved photoluminescence properties of europium complex/polyacrylonitrile composite fibers prepared by electrospinning

Hengguo Wang, Qingbiao Yang*, Lei Sun, Chaoqun Zhang, Yanchun Li, Shuai Wang, Yaoxian Li*

Department of Chemistry, Jilin University, Changchun 130021, PR China

ARTICLE INFO

Article history:
Received 17 June 2009
Received in revised form 1 September 2009
Accepted 2 September 2009
Available online 6 September 2009

Keywords:
Electrospinning
Europium complexes
Polyacrylonitrile (PAN)
Photoluminescence

ABSTRACT

Novel fluorescent composite nanofibers of the europium complexes $Eu(DBM)_3(Bath)$ (DBM = dibenzoylmethanato, Bath = bathophenanthroline) or $Eu(DBM)_3(Phen)$ (Phen = 1,10-phenanthroline) and polyacrylonitrile (PAN) are prepared by electrospinning. The thermal-stability, photo-stability and photoluminescence properties of these composite nanofibers are studied in comparison to that of the pure europium complexes in detail. The results indicate that, after incorporating europium complexes into the polymer matrix, the site symmetry of the coordination sphere for the Eu^{3+} ions decreases, which makes the excitation bands of the composite nanofibers split into two different components. But the PAN can provide a rigid environment for the europium complexes, so the thermal-stability and photo-stability of composite nanofibers are considerably improved. Most importantly, the luminescent quantum efficiency and luminescence lifetime of the composite nanofibers are of great improvement. In addition, compared $Eu(DBM)_3(Bath)$/PAN with $Eu(DBM)_3(Phen)$/PAN composite nanofibers, the former exhibit superior properties.

1. Introduction

Europium complexes have characteristic luminescence properties and give sharp, intense emission lines upon ultraviolet light irradiation due to the effective excitation energy transfer from the surrounding organic ligands to the central metal ions (the so-called antenna effect) [1]. However, they have so far been excluded from practical applications in tunable solid-state laser or phosphor devices because of their poor thermal-stability, low mechanical strength [2] and severe self-quenching [3]. Over the years considerable efforts have been devoted to overcome these shortcomings, including using the sol–gel method and hydrothermal synthesis process to incorporate europium complexes into organic, inorganic and organic/inorganic hybrid matrixes, such as zeolites or mesoporous materials [4–6], sol–gel silica or organically modified silicates (ORMOSIL) [7–10], and polymers [11–15]. However, using a simple and effective method to overcome these shortcomings is still a very challenging task.

Since the first description of an electrospinning setup in 1934 [16], it has proven to be a simple, versatile and cost-effective approach for fabricating long, continuous fibers from a variety of materials, such as polymers [17–20], inorganic [21–24], and hybrid (organic–inorganic) compounds [25–27]. The collected nonwoven fibers show many exciting characteristics such as large surface area to volume ratio, excellent flexibility, and superior mechanical performance. Therefore, the study and utilization of electrospun nanofibers have attracted much attention in recent years. However, electrospinning of nanofibers from europium complex/polymers has not received much attention yet [28–31]. In fact, the electrospinning route, because of the room-temperature synthesis and the europium complexes without suffering thermal degradation, is particularly suitable for incorporation of europium complexes into nanofiber films. The most fascinating advantage of electrospinning is that the polymers used as the matrixes can stabilize the europium complexes [28–30]. As the europium complexes are surrounded with polymers, the stabilization strongly depends on the properties of polymer matrices [30]. Known by their excellent properties of good mechanical strength, thermal-stability and high dielectric constant desirable for electrospinning, polyacrylonitrile (PAN) is an excellent candidates for many potential applications, such as catalyst supports and batteries [32,33].

In this paper, PAN is, for the first time, applied as polymer matrixes to stabilize the europium complexes and electrospun into $Eu(DBM)_3(Bath)$/PAN and $Eu(DBM)_3(Phen)$/PAN composite nanofibers. The photoluminescence properties of europium complex/PAN composite nanofibers are studied in comparison to that of the relevant pure europium complex in detail. It is significant to observe that the thermal-stability, the photo-stability, the fluorescence lifetime and luminescent quantum efficiency of the europium complex composite fibers are of great improvement over that of those pure europium complexes.

* Corresponding authors. Tel.: +86 431 88499845; fax: +86 431 88499845.
E-mail address: yangqb@jlu.edu.cn (Q. Yang).

0925-8388/$ – see front matter © 2009 Elsevier B.V. All rights reserved.
doi:10.1016/j.jallcom.2009.09.002

2. Experimental

2.1. Materials

$Eu(DBM)_3(Phen)$ and $Eu(DBM)_3(Bath)$ were synthesized according to the traditional method described in the literature [34]. Polyacrylonitrile (PAN, M_w = 100,000) was provided by Jilin Chemical Industry Co. (China). And N,N-dimethylformamide (DMF) was supplied by Beijing Chemicals Co. (China). In all experiments, the chemicals were analytical grade and all reagents were used without any further purification.

2.2. Preparation

0.2 g PAN was dissolved in 1.8 g DMF at room temperature, with vigorous stirring for 24 h. Then europium complexes [$Eu(DBM)_3(Phen)$ or $Eu(DBM)_3(Bath)$] were added into the solution with stirring for 2 h, respectively. The above different europium complexes/PAN (3.5 wt% europium complex relative to PAN) homogeneous solutions were formed. The electrospinning procedure reported previously was used to prepare nanofibers. Europium complex/PAN solution was put into a nozzle (the i.d. is 1.2 mm) and electrospun by applying 16 kV at an electrode distance of 18 cm. The fibers were collected on an aluminum frame.

2.3. Characterization

Field emission scanning electron microscope (FESEM, XL30, FEI) and fluorescence microscope (BX51T-3200, Olympus) were applied to observe the morphologies of nanofibers. Thermogravimetric analysis (TGA) was performed on a PerkinElmer Pyris Diamond thermal analyzer up to 1000 °C under nitrogen atmosphere at a heating rate of 10 °C/min. The fluorescence excitation and emission spectra were obtained with a Hitachi F-4500 spectrophotometer equipped with a 150 W xenon lamp as the excitation source. Luminescence lifetimes were measured with 355 nm light from an Nd^{3+}:YAG (yttrium aluminum garnet) laser combined with a third-harmonic generator was used as the pump. An oscilloscope was used to record the decay dynamics.

3. Results and discussion

3.1. Morphology

Fig. 1(A–C) shows FESEM images of the various nanofibers. In all cases (A–C), the nanofibers are randomly oriented on substrate without any evidence of bead-on-string morphology, and their lengths are several millimeters. The average diameters for pure PAN, $Eu(DBM)_3(Phen)$/PAN and $Eu(DBM)_3(Bath)$/PAN nanofibers are ~152, 252 and 292 nm, respectively. It is well known that many factors influence the diameters and morphology of the electrospun nanofibers, such as solution concentration, applied voltage, solution velocity, tip-to-collector distance, and solution properties (polarity, surface tension, and electric conductivity, etc.). Among them, the polymer concentration is a key factor influencing the viscosity of the polymer solution, which plays an important role in the process of electrospinning. So we investigated the viscosity of the solution before and after adding europium complexes. Before adding europium complexes, the viscosity of the PAN/DMF solution is 300 mPa·s. After adding $Eu(DBM)_3(Phen)$ and $Eu(DBM)_3(Bath)$ complexes, the viscosity of the solution is 3300 and 3500 mPa s, respectively. Apparently, with the europium complexes adding to the PAN/DMF solutions, the viscosity of the solutions increased, which lead to the greater nanofiber diameter. The fluorescence microscopy images of europium complexes/PAN composite nanofibers (Fig. 1D and 1E) show bright red emission of $Eu(DBM)_3(Bath)$ and $Eu(DBM)_3(Phen)$, proving that $Eu(DBM)_3(Bath)$ and $Eu(DBM)_3(Phen)$ were capped in the PAN matrix in the nanofibers, respectively.

3.2. Thermogravimetric analysis (TGA)

TGA has been used to characterize the thermal-stability of the all samples. Fig. 2 shows the TGA curves for the all samples. It can be observed that there appeared two steps of weight loss below 1000 °C from composite fibers (Fig. 2B and D). The first step of weight loss below 280 °C is due to the loss of residual solvent [35], and this is followed by a weight loss peak at 540 °C (approximately 28%, Fig. 2B) and at 510 °C (approximately 45%, Fig. 2D) which may be ascribed to the thermal decomposition of composite

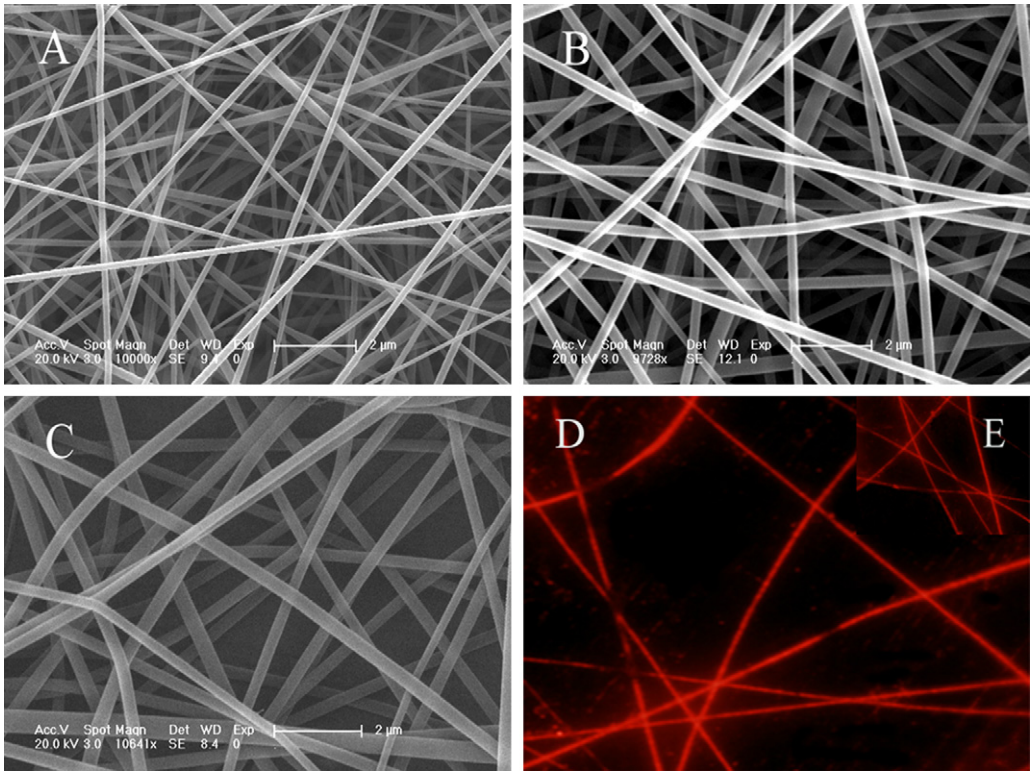

Fig. 1. FESEM images of pure PAN (A), $Eu(DBM)_3(Phen)$/PAN nanofibers (B) and $Eu(DBM)_3(Bath)$/PAN nanofibers (C), and fluorescence microscopy images of $Eu(DBM)_3(Bath)$/PAN nanofibers (D) and $Eu(DBM)_3(Phen)$/PAN nanofibers (E, inset).

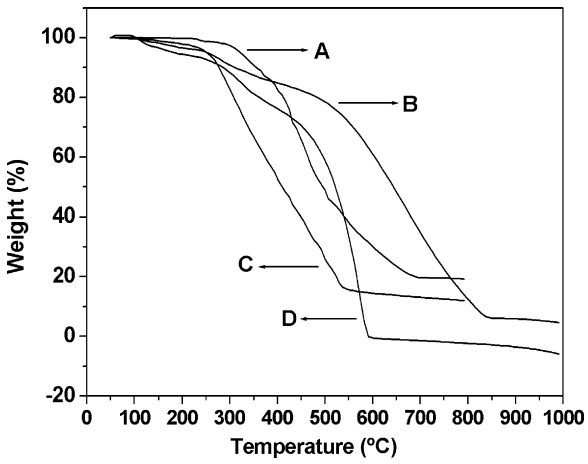

Fig. 2. TGA traces of the pure $Eu(DBM)_3(Bath)$ (A), $Eu(DBM)_3(Bath)$/PAN nanofibers (B), pure $Eu(DBM)_3(Phen)$ (C) and $Eu(DBM)_3(Phen)$/PAN nanofibers (D).

fibers. For pure europium complexes (Fig. 2A and C), the decomposition temperatures are about 350 and 280 °C, respectively. It is obvious that the thermal-stabilities of europium/PAN composite fibers are better than that of the europium complexes. The better thermal-stability can be attributed that the rigid PAN matrixes provide rigid environment for the europium complex, which makes the europium complex more stable. Therefore, in order to improve the thermal-stability of europium complexes, it is a feasible way to use a polymer with good thermal-stability as the matrix. In addition, compared with the weight loss (from 28% to 45%) and T_d (from 540 to 510 °C) of composite fibers, the decomposition point of $Eu(DBM)_3(Bath)$/PAN composite fibers is higher than that of $Eu(DBM)_3(Phen)$/PAN composite fibers, indicating that the former exhibit superior thermal-stability.

Table 1
Photoluminescent data of pure $Eu(DBM)_3(Bath)$ (A), $Eu(DBM)_3(Bath)$/PAN composite fibers (B), pure $Eu(DBM)_3(Phen)$ (C) and $Eu(DBM)_3(Phen)$/PAN composite fibers (D).

Systems	A	B	C	D
υ_{00} (cm^{-1})[a]	17,319	17,325	17,319	17,325
υ_{01} (cm^{-1})[a]	16,982	16,972	16,989	16,700
υ_{02} (cm^{-1})[a]	16,393	16,393	16,399	16,393
υ_{03} (cm^{-1})[a]	15,399	15,427	15,418	15,423
υ_{04} (cm^{-1})[a]	14,294	14,298	14,282	14,314
I_{00}[b]	2,160	468	1,019	543
I_{01}[b]	5,433	1,061	2,582	1,273
I_{02}[b]	56,158	9,165	27,004	10,743
I_{03}[b]	618	99	304	138
I_{04}[b]	189	47	85	41
I_{02}/I_{01}	10.34	8.64	10.46	8.44
τ (ms)[c]	0.29	0.458	0.29	0.424
A_r (s^{-1})	613.1	526.6	619.6	508.3
A_{nr} (s^{-1})	2,835.2	1,658.8	2,828.7	1,850.2
η (%)	17.8	24.1	17.9	21.6

[a] Energies of the $^5D_0$–^7F_J transitions (υ_{0J}).
[b] Integrated intensity of the $^5D_0$–^7F_J emission curves.
[c] For $^5D_0$–^7F_J transition of Eu^{3+}.

3.3. Fluorescence spectrum

The luminescence behaviors of the all samples have been investigated at 298 K. The excitation and emission spectra are given in Fig. 3, and the detailed luminescent data are shown in Table 1.

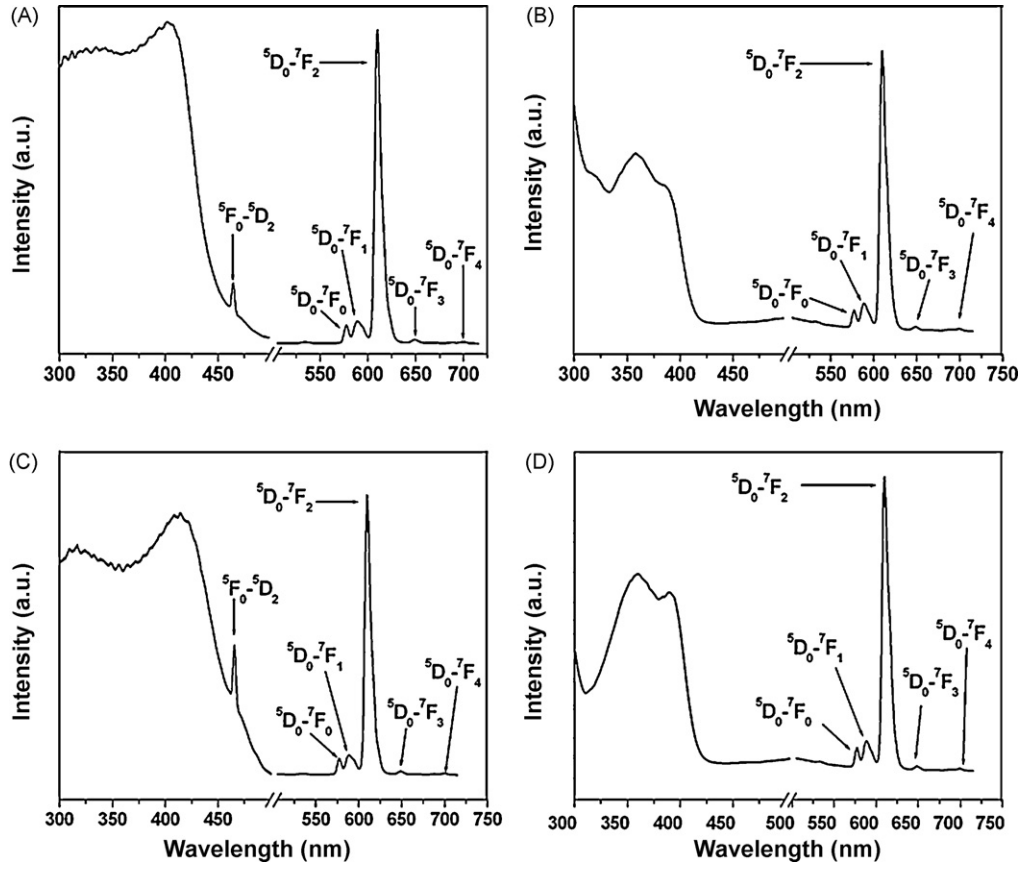

Fig. 3. Excitation spectra (λ_{em} = 610 nm) and emission spectra (λ_{ex} = 365 nm) for the $^5D_0 \rightarrow {}^7F_J$ transitions of Eu^{3+} in pure $Eu(DBM)_3(Bath)$ (A), $Eu(DBM)_3(Bath)$/PAN composite fibers (B), pure $Eu(DBM)_3(Phen)$ (C) and $Eu(DBM)_3(Phen)$/PAN composite fibers (D).

As shown in Fig. 3, every excitation spectra which was obtained by monitoring the emission wavelength of the europium ions at 610 nm exhibits a broad excitation band from 300 to 500 nm, which can be assigned to the π–π^* transitions of conjugated double bonds in the aromatic β-diketonate dibenzoylmethane (DBM) ligands [36]. However, there are two differences between pure complexes and composite fibers. First, the maximum excitation wavelength shifts from 403 to 358 nm for $Eu(DBM)_3(Bath)$ (Fig. 3A and B) and from 412 to 357 nm for $Eu(DBM)_3(Phen)$ (Fig. 3C and D), respectively. The blue shift of the excitation bands ascribes that due to the existence of the surrounding PAN media, the site symmetry of the coordination sphere for the Eu^{3+} ions decreases [37]. Second, in the pure complexes the $^7F_0$–$^5D_2$ excitation line appears, while in the composites the line disappears, which suggests that in the composites the f–f inner-shell transitions are quenched through the nonradiative energy transfer from the higher excited states to some uncertain defect levels, substituting for the nonradiative relaxation to $^5D_0$ [30].

From the emission spectra (Fig. 3A–D), characteristic emission peaks of the europium ion are observed and which are assigned to the transitions $^5D_0 \rightarrow {}^7F_0$ (578 nm), $^5D_0 \rightarrow {}^7F_1$ (590 nm), $^5D_0 \rightarrow {}^7F_2$ (610 nm), $^5D_0 \rightarrow {}^7F_3$ (650 nm) and $^5D_0 \rightarrow {}^7F_4$ (700 nm) with the $^5D_0 \rightarrow {}^7F_2$ transition at 610 nm being the dominant emission peak. As is known, the $^5D_0 \rightarrow {}^7F_1$ transition is a magnetic-dipolar transition and is insensitive to the local structure environment, whereas the $^5D_0 \rightarrow {}^7F_2$ transition is an electric-dipolar transition and is sensitive to the coordination environment of the europium ion. So the intensity (the integration of the luminescent band) ratio of the $^5D_0 \rightarrow {}^7F_2$ transition to the $^5D_0 \rightarrow {}^7F_1$ transition can be used as a reference to compare different chemical environment of europium complex, that is, it can be used as an indicator of Eu^{3+} site symmetry [38]. The $^5D_0 \rightarrow {}^7F_2/{}^5D_0 \rightarrow {}^7F_1$ intensity ratios for all materials are listed in Table 1. These results suggest that, incorporating $Eu(DBM)_3(Bath)$ and $Eu(DBM)_3(Phen)$ into PAN decreases the symmetry of the coordination environment for Eu^{3+} ions.

3.4. Photoluminescence stability

The instability of rare complexes under UV irradiation is one of the problems for their practical application. To compare the photoluminescence stability of the electrospun nanofibers with that of the pure europium complexes, ultraviolet light irradiation induced spectral changes were studied and the decay curves of the $^5D_0 \rightarrow {}^7F_2$ emission band as a function of irradiation time were given in Fig. 4. As shown in Fig. 4, the emission intensity in the pure complexes (A and C) decreases remarkably with the increasing exposure time, whereas in the composite nanofibers (B and D) the fluorescence intensity is weakened with a slower rate of decline than for pure complexes. So incorporating europium complexes into PAN electrospun nanofibers could improve the photoluminescence stability under UV irradiation. The possible reason is that the PAN polymer can provide a more relatively rigid environment for the complexes to reduce the energy consumption on vibration of ligands and intermolecular collision of the complexes [30]. Thus, the PAN matrixes can protect the complexes from decomposing under UV irradiation. In addition, compared the photoluminescence stability of the $Eu(DBM)_3(Bath)$/PAN nanofibers with that of $Eu(DBM)_3(Phen)$/PAN nanofibers, the former exhibits superior photoluminescence stability.

3.5. Luminescence decay times and luminescent quantum efficiency

Fig. 5 shows the time-resolved intensity-decay curves for the various samples monitored at the $^5D_0 \rightarrow {}^7F_2$ transition (610 nm) of Eu^{3+} ion at room temperature. The fitting parameters of these decay

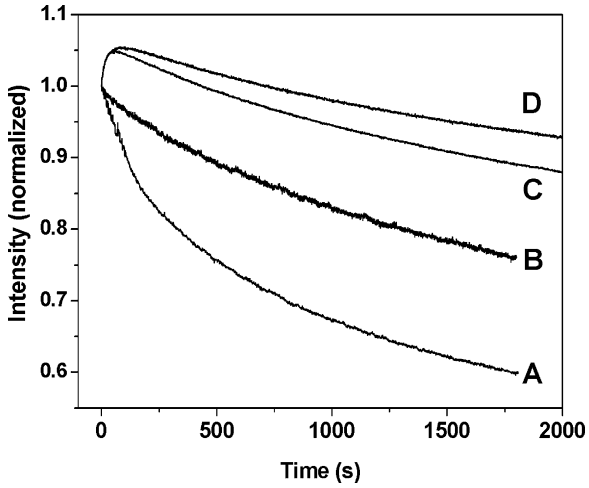

Fig. 4. Dependence of normalized intensity at 610 nm on irradiation time in pure $Eu(DBM)_3(Bath)$ (A), pure $Eu(DBM)_3(Phen)$ (B), $Eu(DBM)_3(Phen)$/PAN nanofibers (C) and $Eu(DBM)_3(Bath)$/PAN nanofibers (D). The samples were irradiated with 355 nm light.

curves are summarized in Table 2. These results clearly show that the time-resolved intensity decay of the pure europium complexes could be fitted to a single-exponential decay curve. However, the time-resolved intensity decay of the composite nanofibers could be fitted very well to bi-exponential decay curve [39]. And it is obvious that the fluorescent lifetimes of composite fibers increase significantly as compared with the pure europium complexes. Besides, the lifetime of $Eu(DBM)_3(Bath)$/PAN composite fibers is much higher than that of $Eu(DBM)_3(Phen)$/PAN composite fibers. All these data indicate that when the europium complexes are dispersed in the PAN matrixes, the matrixes may bestow a certain degree of protection on the europium complexes and organic polymeric chain can enhance the luminescence stability of the europium complexes [40].

In fact, the lifetime of $^5D_0$, τ is dominated by the radiative transition rate of $^5D_0 \rightarrow \sum {}^7F_J$, A_r, and the nonradiative decay rate A_{nr}, which can be written as: [10,38,41–47]

$$\tau_{exp} = (A_r + A_{nr})^{-1} \quad (1)$$

Here A_r can be obtained by summing over the radiative rates A_{0J} for each $^5D_0 \rightarrow {}^7F_J$ transitions of Eu^{3+} [10,38,41–47].

$$A_r = \sum A_{0J} = A_{00} + A_{01} + A_{02} + A_{03} + A_{04} \quad (2)$$

The branching ratio for the $^5D_0 \rightarrow {}^7F_5$ and $^5D_0 \rightarrow {}^7F_6$ transitions must be neglected as they are not detected experimentally. Therefore, we can ignore their influence in the depopulation of the $^5D_0$ excited state [10,38,41–47].

As mentioned previously, since the $^5D_0 \rightarrow {}^7F_1$ transition is a magnetic-dipolar transition and is insensitive to the local structure environment around the Eu^{3+} ion, and thus can be considered as an internal reference for the whole spectrum, the experimental coefficients of spontaneous emission, A_{0J} can be calculated according to the equation [10,38,41–47].

$$A_{0J} = A_{01}\left(\frac{I_{0J}}{I_{01}}\right)\left(\frac{\upsilon_{01}}{\upsilon_{0J}}\right) \quad (3)$$

where υ_{01} and υ_{0J} are the energy baricenters of the $^5D_0 \rightarrow {}^7F_1$ and $^5D_0 \rightarrow {}^7F_J$ transitions, respectively [45]. A_{01} is the Einstein's coefficient of spontaneous emission between the $^5D_0$ and $^7F_1$ energy levels. Since in vacuum, the value of A_{01} can be determined to be $50\ s^{-1}$ approximately ($A_{01} = n^3 A_{01}$ (vacuum)) [38,46]. I is the emission intensity and can be taken as the integrated intensity of the

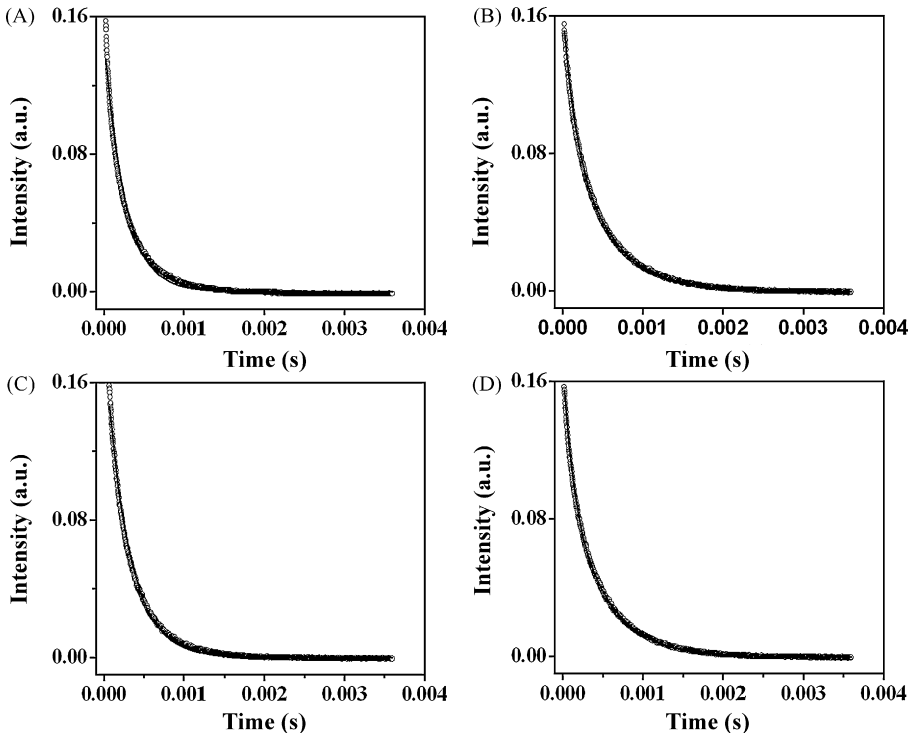

Fig. 5. Fluorescence decay curves of the $^5D_0 \rightarrow {}^7F_2$ transitions (λ_{em} = 610 nm) in pure Eu(DBM)$_3$(Bath) (A), Eu(DBM)$_3$(Bath)/PAN nanofibers (B), pure Eu(DBM)$_3$(Phen) (C) and Eu(DBM)$_3$(Phen)/PAN nanofibers (D). Fit to a single-exponential or bi-exponential decay model is shown (solid line).

$^5D_0 \rightarrow {}^7F_J$ emission bands [10,47]. Here the emission intensity, I, taken as integrated intensity S of the $^5D_0 \rightarrow {}^7F_{0-4}$ emission curves, can be defined as below:

$$I_{i-j} = \hbar\omega_{i-j}A_{i-j}N_i \approx S_{i-j} \quad (4)$$

where i and j are the initial ($^5D_0$) and final levels ($^7F_{0-4}$), respectively, ω_{i-j} is the transition energy, A_{i-j} is the Einstein's coefficient of spontaneous emission, and N_i is the population of the $^5D_0$ emitting level.

Assuming that only nonradiative and radiative processes are essentially involved in the depopulation of the $^5D_0$ state, η can be defined as follows [10,38,41–47].

$$\eta = \frac{A_r}{A_r + A_{nr}} \quad (5)$$

So according to the radiative transition rate constant and experimental luminescence lifetime, quantum efficiency can be calculated from the following equation

$$\eta = A_r\,\tau_{exp} \quad (6)$$

On the basis of the above discussion, it can be seen the value η mainly depends on the values of two quanta: one is lifetime and the other is I_{02}/I_{01}. According to the emission spectra and lifetimes of the $^5D_0$ emitting level, the emission quantum efficiency (η) of the $^5D_0$ Eu^{3+} excited state can be determined and the detailed luminescent data were shown in Table 1. As shown in Table 1, the quantum efficiencies of pure europium complex and composite nanofibers can be determined in the following order: Eu(DBM)$_3$(Bath)/PAN composite fibers > pure Eu(DBM)$_3$(Bath) and Eu(DBM)$_3$(Phen)/PAN composite fibers > pure Eu(DBM)$_3$(Phen), which are in agreement with the order of lifetimes. In addition, compared with the quantum efficiency of composite fibers, the quantum efficiency of Eu(DBM)$_3$(Bath)/PAN composite fibers is higher than that of Eu(DBM)$_3$(Phen)/PAN composite fibers, indicating that the former exhibit superior luminescence properties.

Table 2
Time-resolved intensity-decay constants for pure Eu(DBM)$_3$(Bath) (A), Eu(DBM)$_3$(Bath)/PAN composite fibers (B), pure Eu(DBM)$_3$(Phen) (C) and Eu(DBM)$_3$(Phen)/PAN composite fibers (D).

Systems	A	B	C	D
α_1	0.128	0.109	0.185	0.056
τ_1 (ms)	0.29	0.5	0.2	0.10
α_2		0.054		0.112
τ_2 (ms)		0.13		0.46
τ (ms)	0.29	0.458	0.29	0.424
R^2	0.9967	0.9998	0.9968	0.9998

4. Conclusions

We successfully prepared fluorescent europium complex/PAN composite nanofibers by electrospinning. Owing to incorporating a polymer with good mechanical strength, thermal-stability and high dielectric constant desirable for electrospinning, the photoluminescence properties of europium complex/PAN composite fibers were improved considerably in comparison to that of the pure europium complex. The PAN polymer provides a rigid environment to protect the pure europium complex from decomposing under UV irradiation and high temperature. So the thermal-stability and photo-stability of europium complex/PAN composite fibers are much better than that of the pure europium complexes. Most importantly, the luminescent quantum efficiency and luminescence lifetime of the composite nanofibers are of great improvement. Thus PAN is an ideal polymer matrix to stabilize europium complexes. In addition, compared with the Eu(DBM)$_3$(Bath)/PAN and Eu(DBM)$_3$(Phen)/PAN composite nanofibers, the former exhibit superior properties than the latter. The improvement of the properties, and the simple and versatile preparing method endow europium complex/PAN composite nanofibers with the potential application in tunable solid-state laser or phosphor devices.

Acknowledgment

The authors gratefully acknowledge the support of the National Natural Science Foundation of China (No. 20674023).

References

[1] S.I. Weissman, J. Chem. Phys. 10 (1942) 214.
[2] D.W. Dong, S.C. Jiang, Y.F. Men, X.L. Ji, B.Z. Jiang, Adv. Mater. 12 (2000) 646.
[3] K. Binnemans, P. Lenaerts, K. Driesen, C. Gorller-Walrand, J. Mater. Chem. 14 (2004) 191.
[4] H.H. Liu, H.W. Song, S.W. Li, X.G. Ren, S.Z. Lu, H.Q. Yu, G.H. Pan, H. Zhang, L.Y. Hu, Q.L. Dai, R.F. Qin, J.H. Yu, G.M. Wang, J.X. Jiang, J. Nanosci. Nanotechnol. 8 (2008) 3959.
[5] Y. Chen, Q. Chen, L. Song, H.P. Li, F.Z. Hou, Microporous Mesoporous Mater. 122 (2009) 7.
[6] S.J. Seo, D. Zhao, K. Suh, J.H. Shin, B.S. Bae, J. Lumin. 128 (2008) 565.
[7] L.L. Kong, B. Yan, Y. Li, J. Alloys Compd. 481 (2009) 549.
[8] J.L. Liu, B. Yan, J. Phys. Chem. B 112 (2008) 10898.
[9] Y. Li, B. Yan, H. Yang, J. Phys. Chem. C 112 (2008) 3959.
[10] C.Y. Peng, H.J. Zhang, J.B. Yu, Q.G. Meng, L.S. Fu, H.R. Li, L.N. Sun, X.M. Guo, J. Phys. Chem. B 109 (2005) 15278.
[11] S.T. Tan, X.M. Feng, B. Zhao, Y.P. Zou, X.W. Huang, Mater. Lett. 62 (2008) 2419.
[12] R. Shunmugam, G.N. Tew, Macromol. Rapid Commun. 29 (2008) 1355.
[13] W.Y. Lai, J.W. Levell, P.L. Burn, S.C. Lo, I.D.W. Samuel, J. Mater. Chem. 19 (2009) 4952.
[14] X.F. Qiao, B. Yan, Inorg. Chem. 48 (2009) 4714.
[15] C.Y. Yang, V. Srdanov, M.R. Robinson, G.C. Bazan, A.J. Heeger, Adv. Mater. 14 (2002) 980.
[16] A. Formhals, US Patent No. 1,975,504 (1934).
[17] Y. Il Yoon, H.S. Moon, W.S. Lyoo, T.S. Lee, W.S. Park, J. Colloid Interface Sci. 320 (2008) 91.
[18] M. Bognitzki, W. Czado, T. Frese, A. Schaper, M. Hellwig, M. Steinhart, A. Greiner, J.H. Wendorff, Adv. Mater. 13 (2001) 70.
[19] S. Madhugiri, A. Dalton, J. Gutierrez, J.P. Ferraris, K.J. Balkus, J. Am. Chem. Soc. 125 (2003) 14531.
[20] L. Yao, T.W. Haas, A. Guiseppi-Elie, G.L. Bowlin, D.G. Simpson, G.E. Wnek, Chem. Mater. 15 (2003) 1860.
[21] S.H. Zhan, D.R. Chen, X.L. Jiao, S.S. Liu, J. Colloid Interface Sci. 308 (2007) 265.
[22] D. Li, Y.N. Xia, Nano Lett. 3 (2003) 555.
[23] H.Q. Hou, D.H. Reneker, Adv. Mater. 16 (2004) 69.
[24] J.G. Zhao, C.W. Jia, H.G. Duan, Z.W. Sun, X.M. Wang, E.Q. Xie, J. Alloys Compd. 455 (2008) 497.
[25] J.J. Ge, H. Hou, Q. Li, M.J. Graham, A. Greiner, D.H. Reneker, F.W. Harris, S.Z.D. Cheng, J. Am. Chem. Soc. 126 (2004) 15754.
[26] M.M. Demir, M.A. Gulgun, Y.Z. Menceloglu, B. Erman, S.S. Abramchuk, E.E. Makhaeva, A.R. Khokhlov, V.G. Matveeva, M.G. Sulman, Macromolecules 37 (2004) 1787.
[27] J. Li, E.H. Liu, W. Li, X.Y. Meng, S.T. Tan, J. Alloys Compd. 478 (2009) 371.
[28] H. Zhang, H.W. Song, H.Q. Yu, X. Bai, S.W. Li, G.H. Pan, Q.L. Dai, T. Wang, W.L. Li, S.Z. Lu, X.G. Ren, H.F. Zhao, J. Phys. Chem. C 111 (2007) 6524.
[29] H. Zhang, H.W. Song, H.Q. Yu, S.W. Li, X. Bai, G.H. Pan, Q.L. Dai, T. Wang, W.L. Li, S.Z. Lu, X.G. Ren, H.F. Zhao, X.G. Kong, Appl. Phys. Lett. 90 (2007) 103103.
[30] H. Zhang, H.W. Song, B. Dong, L.L. Han, G.H. Pan, X. Bai, L.B. Fan, S.Z. Lu, H.F. Zhao, F. Wang, J. Phys. Chem. C 112 (2008) 9155.
[31] Q.C. Liu, B. Li, J. Gong, Y.L. Sun, W.L. Li, J. Alloys Compd. 466 (2008) 314.
[32] J.T. McCann, B.K. Lim, R. Ostermann, M. Rycenga, M. Manque, Y.N. Xia, Nano Lett. 7 (2007) 2470.
[33] C. Kim, K.S. Yang, M. Kojima, K. Yoshida, Y.J. Kim, Y.A. Kim, M. Endo, Adv. Funct. Mater. 16 (2006) 2393.
[34] P.S. Chowdhury, S. Saha, A. Patra, Chem. Phys. Lett. 405 (2005) 393.
[35] H. Dong, S. Prasad, V. Nyame, W.E. Jones, Chem. Mater. 16 (2004) 371.
[36] S. Moynihan, D. Iacopino, D. O'Carroll, H. Doyle, D.A. Tanner, G. Redmond, Adv. Mater. 19 (2007) 2474.
[37] N.C. Chang, J.B. Gruber, J. Chem. Phys. 41 (1964) 3227.
[38] O.L. Malta, H.F. Brito, J.F.S. Menezes, F.R. Goncalves e Silva, S. Alves, F.S. Farias, A.V.M. DeAndrade, J. Lumin. 75 (1997) 255.
[39] M.T. Murtagh, M.R. Shahriari, M. Krihak, Chem. Mater. 10 (1998) 3862.
[40] Y. Bing, X.F. Qiao, J. Phys. Chem. B 111 (2007) 12362.
[41] O.L. Malta, M.A. Couto dos Santos, L.C. Thompson, N.L. Ito, J. Lumin. 69 (1996) 77.
[42] L.D. Carlos, Y. Messaddeq, H.F. Brito, R.A. Sa Ferreira, V. De Zea Bermudez, S.J.L. Ribeiro, Adv. Mater. 12 (2000) 594.
[43] R.A. Sa'Ferreira, L.D. Carlos, R.R. Goncalves, S.J.L. Ribeiro, V. De Zea Bermudez, Chem. Mater. 13 (2001) 2991.
[44] P.C.R. Soares-Santos, H.I.S. Nogueira, V. Felix, M.G.B. Drew, R.A. Sa Ferreira, L.D. Carlos, T. Trindade, Chem. Mater. 15 (2003) 100.
[45] E.E.S. Teotonio, J.G.P. Espinola, H.F. Brito, O.L. Malta, S.F. Oliveria, D.L.A. De Foria, C.M.S. Izumi, Polyhedron 21 (2002) 1837.
[46] S.J.L. Ribeiro, K. Dahmouche, C.A. Ribeiro, C.V. Santilli, S.H. Pulcinelli, J. Sol–Gel Sci. Technol. 13 (1998) 427.
[47] M.H.V. Werts, R.T.F. Jukes, J.W. Verhoeven, Phys. Chem. Chem. Phys. 4 (2002) 1542.